UNIVERSITY OF ILLINOIS AT URBANA-CHAMPAIGN

THE GRADUATE COLLEGE

DECEMBER 2000

WE HEREBY RECOMMEND THAT THE THESIS BY

ALEX TAN KWAN

ENTITLED NANO-SCALE CALORIMETRY OF ISOLATED POLYETHYLENE SINGLE CRYSTALS

BE ACCEPTED IN PARTIAL FULFILLMENT OF THE REQUIREMENTS FOR THE DEGREE OF MASTER OF SCIENCE

Leslie Allen

Director of Thesis Research

Head of Department

Committee on Final Examination†

Chairperson

† Required for doctor's degree but not for master's.

O-517

copy

NANO-SCALE CALORIMETRY OF ISOLATED POLYETHYLENE SINGLE CRYSTALS

BY

ALEX TAN KWAN

B.S., Stanford University, 1998

THESIS

Submitted in partial fulfillment of the requirements
for the degree of Master of Science in Materials Science and Engineering
in the Graduate College of the
University of Illinois at Urbana-Champaign, 2001

Urbana, Illinois

ABSTRACT

By using a Micro-Electro-Mechanical System (MEMS) device, the nanocalorimeter, it was possible to investigate the melting of isolated polyethylene (PE) single crystals grown from solution. Atomic force microscopy (AFM) was used to obtain an idea of the morphology and to determine thickness measurements. Transmission electron microscopy (TEM) was used to obtain an idea of the crystallinity of the system. Preliminary work involved the use of a macro-scale system, a simple Ni-foil calorimeter, to measure the heat capacity of a thin polyethylene film to verify if the technique is feasible on the nano-scale. With the nanocalorimeter, it was possible to observe the melting of as few as 25 PE single crystals with lamella thicknesses of 12 ± 1 nm. Over a wide number of crystals (25-2000 crystals), the heat of fusion is found to be 198 J/gm, 40% larger than the bulk value. The melting temperature of the isolated single crystals is 123 ± 2 °C, nine degrees below that of the bulk material. The heat of fusion of quenched crystals was measured to be ± 15% over a wide range of heating rates (20,000-100,000 K/s). Annealing the quenched crystals results in shifts in the endotherm peak by as much as 15 ^{o}C.

DEDICATION

I dedicate this work to my father, Dan Kwan, my mother, May Kwan, and my sister, Lisa Kwan. Their support and love brought me through the past two and a half years of my studies here at the University of Illinois.

ACKNOWLEDGEMENTS

I gratefully acknowledge and thank all the members of Professor Les Allen's research group, Dr. Michael Efremov, Ming Zhang, Eric Olson, Dr. Francois Schiettekatte, and Jeremy Warren. I learned a great deal from these great scientists and engineers that surrounded me. This work would not have been possible without their time, efforts, and insights. I gratefully thank Professor Les Allen for teaching and guiding me in this work and opening my eyes to the wonders and realities of science. It was a pleasure and honor participating in the work of nanocalorimetry. I gratefully thank Professor Phil Geil for his insight and discussion regarding polyethylene single crystals. I also am thankful for the University of Illinois for its facilities and faculty. The Lord of Life, Jesus Christ, has blessed me with many lessons and good things these past two and a half years. I thank Him for His provisions.

TABLE OF CONTENTS

I. INTRODUCTION

This millennium will be marked by major advances in polymer science, spearheaded in part by gains made in manipulating and characterizing material on the nano-scale. Ideas such as self-assembly of macromolecules and nanostructure engineering have generated a critical need to probe material on the length scale of molecules (nanometers). Fortunately, the frontiers of nanometer scale characterization are being rapidly pushed forward with the invention of new "tools" being developed in the field of Micro-Electro-Mechanical Systems (MEMS). Nanocalorimetry is one such tool developed in our group and is capable of probing material at the nano-scale level. This MEMS tool essentially measures temperature and small amounts of heat in order to quantify the thermal properties of materials (melting point, latent heat, heat capacity, etc.). The device, the nanocalorimeter, is specifically constructed to have a small thermal mass and is intended to undergo fast heating rates to achieve such measurements. This thesis focuses on the first steps in introducing the nanocalorimeter to polymer science by studying isolated polyethylene (PE) single crystals grown from a dilute solution – the model crystalline polymer system.

Polyethylene is the model crystalline system in polymer science and yet there still remain important issues, which cannot be addressed via conventional calorimetry. These include the variations of melting point (T_m) as a function of both initial thickness[1] and thermal cycling history.[2] PE single crystals are metastable – they reorganize and recrystallize during the process of the calorimetry scan itself.[3,4,5] Furthermore, the crystals also tend to thicken during heating.[6]

An ideal sample configuration would have PE single crystals, grown from solution, sprayed onto a thin substrate. After the solvent vaporizes the residual PE crystals lie flat on the substrate and are isolated from one another. Isolation limits any interactions between the crystals, allows convenient thickness measurements using atomic force microscopy (AFM) and permits diffraction on individual crystals to be taken with a transmission electron microscope (TEM).

Such a sample configuration is not possible with conventional differential scanning calorimetry (DSC), intended for macro-scale samples. So the DSC does not have the sensitivity needed to detect a small enough number of PE single crystals so that they are isolated. Thus, macro-scale DSC has been limited to sample sizes no smaller than a fraction of a milligram.[7,8]

Our nanocalorimeter has several advantages over conventional DSC in regards to studying PE single crystals. First, by reducing overall thermal mass of the calorimetric system (much smaller than DSC), it becomes very sensitive. Our device is sensitive to the nanojoule level,[9] which corresponds to approximately hundreds of picograms of PE single crystals (~25 individual crystals). Second, by employing very fast scan rates (up to 1,000,000 K/s) during calorimetric measurements, recrystallization before melting is inhibited. The scan rates we employ, 10^4 - 10^5 K/s, are three orders of magnitude greater than those used in optical microscopy experiments, which were able to detect melting at fast heating rates (2 - 33 K/s).[10] In addition, because of the intimate thermal contact between the sample and heater-thermometer in our design, the problem of thermal lag is drastically reduced. Lastly, the nanocalorimeter is constructed using a thin silicon nitride

membrane as a sample holder. This membrane is an ideal substrate for isolated PE single crystals to observe with AFM and TEM.

In this thesis, I will first present an introduction to the study of PE single crystals grown from solution and the technique of nanocalorimetry. Following this introduction, I will describe the various tools and methods used to conduct my studies on the nano-scale calorimetry of PE single crystals. I will proceed to discuss my results, discuss possible future work, and conclude with a short summary.

List of References

[1] Zhou, H.; Wilkes. G. L., Polymer 1997, 38, 5735.

[2] Snyder, R. G.; Scherer, J. R.; Reneker, D. H.; Colson, J. P., Polymer 1982, 23, 1286.

[3] Grubb, D.T.; Liu, J. J-H.; Caffrey, M.; Bilderback, D. H., J. Polym. Sci. Polym. Phys. 1984, 22, 367.

[4] Kawaguchi, A.; Ichida, T.; Murakami, S.; Katayama, K., Colloid. Polym. Sci. 1984, 262, 597.

[5] Mandelkern, L; Sharma, R. K.; Jackson, J. F., Macromolecules 1969, 2, 644.

[6] Magill, J. H., J. Polym. Sci. Polym. Lett. Ed. 1982, 20, 1.

[7] Van Oort, M. J. M.; White, M. A., Rev. Sci. Instrum. 1987, 58, 1239.

[8] Pecharsky, V. K.; Moorman, J. O.; Gschneidner, K. A. Jr., Rev. Sci. Instrum. 1997, 68, 4196.

[9] Lai, S. L.; Guo, J. Y.; Petrova, V; Ramanath, G.; Allen, L. H., Phys. Rev. Lett. 1996, 77, 99.

[10] Hellmuth E.; Wunderlich, B., J. Appl. Phys. 1965, 36, 3039.

II. BACKGROUND

II.1. Polyethylene Single Crystals

Polyethylene is an organic polymer, which means that it is an organic long-chain molecule made up of repeating units that are connected by covalent bonds. Its main repeating unit, also termed monomer, is the ethylene group ($-CH_2-$). Depending on how it is synthesized, polyethylene can have molecular weights between several thousand and several million. In its linear form, there is no branching, that is no side chains in the structure. Typically, a polymer is not extended which would not allow any interactions to occur between non-neighboring units. Rather, secondary bonds occur, which are weaker than covalent bonds, like van der Waals forces or hydrogen bonds, which results in attractive forces between non-neighboring units. It is these secondary bonds that result in the molecules crystallizing. A more in-depth discussion may be found in Geil's book, *Polymer Single Crystals*.[1]

The growth and identification of lamella single crystals of linear polyethylene from solution was first reported in 1957 by Till[2], Keller[3], and Fischer[4]. PE single crystals grown from dilute solution have lateral dimensions of several microns and thickness of several nanometers. In the crystals, the polyethylene chains are almost normal with respect to the lamellae's surface. The chain lengths of polyethylene are several orders of magnitude larger than the lamella thickness and thus are folded within the crystal. Figure 2.1 is a cartoon of the system for better visualization. Early work used electron microscopy to understand the structure of the crystals.[5] It was found that the growth faces are the {110} planes.

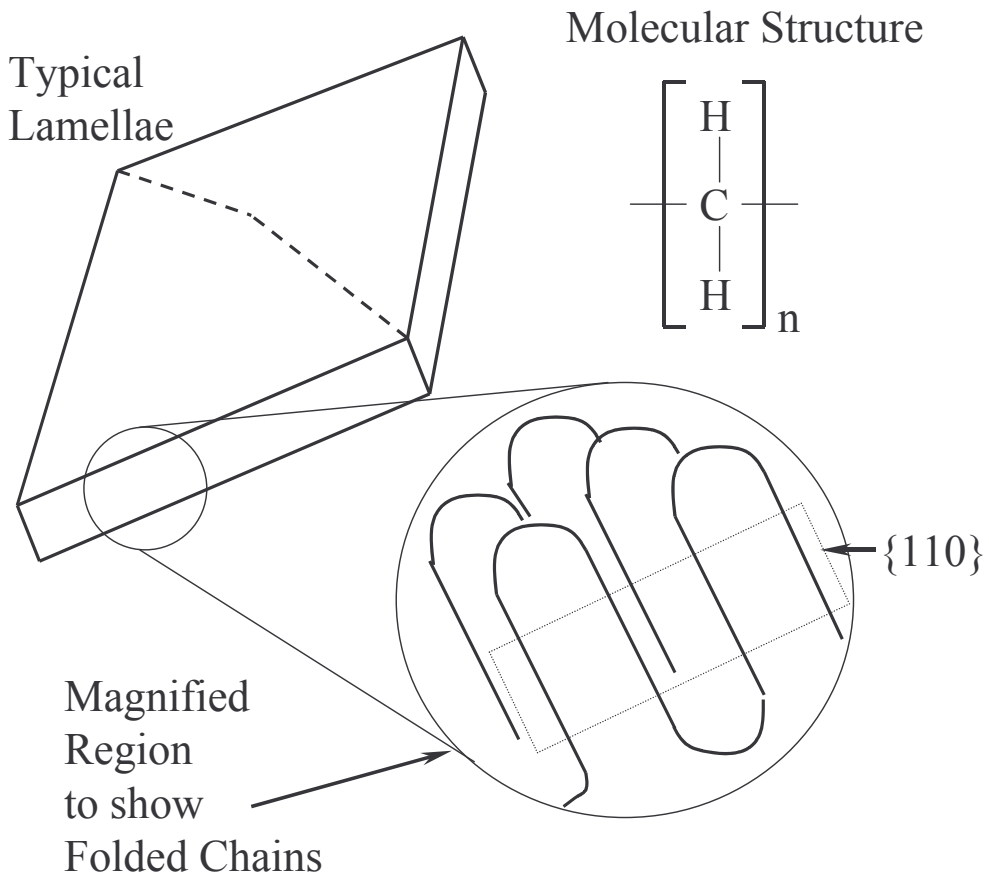

Figure 2.1. A cartoon of a PE single crystal. The polymer chains follow a folded configuration and are oriented normal to the lamellae surface. Typical crystals also assume a pyramidal shape as expressed by the dashed lines. Also shown is the molecular structure where n indicates the number of repeating units.

It was also found that the thermal history of the solution, choice of solvent, concentration, and molecular weight all had a significant effect on the structure and shape of the crystals.[6,7] The thermal properties of the crystals were also studied using DSC and other techniques.[8,9] Past work also included the analysis of annealed single crystals using X-ray techniques,[10], Raman spectroscopy[11], and neutron scattering.[12] It would be of much interest to study the annealed crystals by using our technique. In this thesis, I only present the calorimetry of as-deposited and annealed, quenched PE single crystals grown from solution.

II.2. Nanocalorimetry

The two key features of the technique include the reduction of the overall thermal mass[13,14] of the calorimetry system and the use of a fast scan rate. The ability to measure small amounts of heat depends on the relative heat capacity of the entire calorimetry apparatus. The scan rate in calorimetry is important because sensitivity is related to the heat loss during the measurement.

By using standard thin film processing technology at the Cornell Nanofabrication Facility, it is possible to combine the components typically found in conventional calorimetry systems, namely the sample holder, the heater, and the thermometer, into a single mulitlayer thin film configuration. The sample holder is a low-stress silicon nitride membrane supported at the perimeter by a silicon substrate. A metal strip is deposited on the membrane and functions as the heater and thermometer.

Lai first used this system to study the size-dependent melting point depression of thin films of Sn and Al.[15] Recently, Olson continued the use of this technique to study the vaporization of nanoliter water droplets.[16] Also recently, Efremov, Zhang, and Schiettekatte used this technique and observed size-dependent melting point depression

and the discrete magic nature of indium nanostructures.[17,18] Previously, other techniques, similar in nature to the present version of nanocalorimetry, have been used to study thin films[19], nano-gram amounts of *n*-alkanes[20], and individual superconductor crystals.[21,22] No work has been done to our knowledge on the investigation of polymer single crystals with nanocalorimetry.

List of References

[1] Geil, P. H. In Polymer Single Crystals; John Wiley and Sons: New York, 1963; p 3.

[2] Till, P.H., J. Polymer Sci. 1957, 24, 301.

[3] Keller, A., Phil. Mag. 1957, 2, 1171.

[4] Fischer, E.W., Z. Naturforsch., 1957, 12a, 753.

[5] Geil, P.H. In Polymer Single Crystals; John Wiley and Sons: New York, 1963; p 85.

[6] Leung, W.M.; Manley, R.St.J.,; Panaras, A.R., Macromolecules 1985, 18, 746.

[7] Cooper, M.; Manley, R. St. J., Macromolecules 1975, 8, 219.

[8] Mandelkern, L.; Prasad, A.; Alamo, R.G.; Stack, G.M., Macromolecules 1990, 23, 3696.

[9] Hellmuth E.; Wunderlich, B., J. Appl. Phys. 1965, 36, 3039.

[10] Weaver, T. J.; Harrison, I. R., Polymer 1981, 22, 1590.

[11] Snyder, R. G.; Scherer, J. R.; Reneker, D. H.; Colson, J. P., Polymer 1982, 23, 1286.

[12] Sadler, D. M.; Spells, S. J., Macromolecules 1989, 22, 3941.

[13] Randzio, S.; Zielenkiewicz, W., Phys. Chem. 1976, XXIV, 323.

[14] Borroni-Bird, C.E.; King, D.A., Rev. Sci. Instrum. 1991, 62, 2177.

[15] Lai, S.L., Ph.D. thesis, University of Illinois Urbana-Champaign 1998.

[16] Olson, E. A.; Efremov, M. Y.; Kwan, A. T.; Lai, S.; Petrova, V.; Schiettekatte, F.; Warren, J. T.; Zhang, M.; Allen, L. H., Appl. Phys. Lett. 2000, 77, 2671.

[17] Zhang, M.; Efremov, M.Yu.; Schiettekatte, F.; Olson, E.A.; Kwan, A.T.; Lai, S.L.; Wisleder, T.; Greene, J.; Allen, L.H., Phys. Rev. B 2000, 62, 10548.

[18] Efremov, M. Y.; Schiettekatte, F.; Zhang, M.; Olson, E. A.; Kwan, A. T.; Berry, R. S.; Allen, L. H. Phys. Rev. Lett. 2000, 85, 3560.

[19] Denlinger, D. W.; Abarra, E. N.; Allen, K.; Rooney, P. W.; Messer, M. T.; Watson, S. K.; Hellman, F. Rev. Sci. Instrum. 1994, 65, 946.

[20] Nakagawa, Y.; Schäfer, R.; Güntherodt, H.-J., Appl. Phys. Lett. 1998, 73, 2296.

[21] Fominaya, F.; Fournier, T.; Gandit, P.; Chaussy, J., Rev. Sci. Instrum. 1997, 68, 4191.

[22] Riou, O.; Gandit, P.; Charalambous, M.; Chaussy, J., Rev. Sci. Instrum. 1997, 68, 1501.

III. EXPERIMENTAL

III.1. Preliminary Ni foil Device

As a preliminary experiment to demonstrate the feasibility of obtaining calorimetric data by a metal resistance heater/thermometer structure, we used a free-standing 6 μm thick Ni foil strip shown in Figure 3.1. The system is very simple but the ideas from experiment are the groundwork for actual operation of the nanocalorimeter. The nanocalorimeter is essentially a miniaturized version (fabricated by standard silicon micromachining processes) of the Ni-foil structure.

Because nickel is a metal and has a positive temperature coefficient of resistance (TCR), it is possible to find the relationship between temperature and resistance by using a hot plate and a calibrated thermocouple. Calorimetric data was obtained by heating a 24 μm thick polyethylene film with a 6 μm thick Ni foil. The measurement is initiated by supplying a short (~1 second) dc current pulse to the Ni heater, thus raising the temperature of the system by Joule heating. The voltage and current are monitored in real time during the pulse and thus the power supplied to the system is obtained directly (P = VI). During the pulse, changes in resistance (R = V/I) can be determined in real time as well. In order to evaluate the data in terms of standard thermodynamic parameters, the raw data is evaluated in terms of heat capacity C_p. This is obtained from the data using the following expression:

$$C_p = \frac{dQ/dt}{dT/dt} = \frac{V(t)\cdot I(t)}{dT/dt}. \quad (1)$$

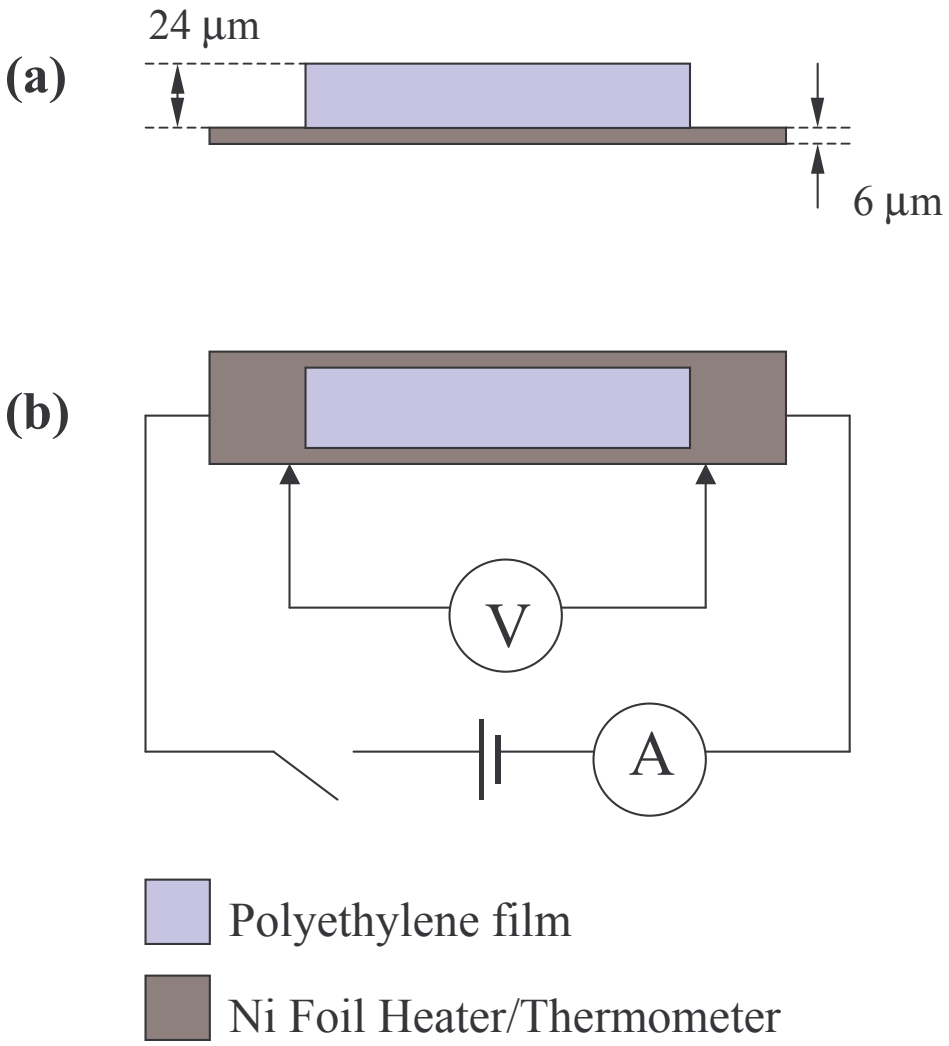

Figure 3.1. Cross-sectional (a) and planar (b) view of the Ni foil calorimeter. The Ni foil strip functions as both the heater and thermometer. The sample, a polyethylene film, rests on top of the Ni. Calorimetric measurements are made by passing a short current pulse through the foil and monitoring the voltage in real time. Voltage and current measurements determine both the power dissipated and temperature.

A temperature scan must be performed without the sample first. The sample is then added to the Ni foil and another measurement is performed. The difference in heat capacity data for the two measurements will be the heat capacity of the polyethylene film. The design of the measurement system allows for a sample size comparable to that of traditional differential scanning calorimetry (DSC) methods. A direct comparison to accepted calorimetry methods is thus possible.

III.2. Fabrication of the Nanocalorimeter

The steps involved in the fabrication of the Joule heating nanocalorimeter are shown in Figure 3.2. The structure and method of fabrication are similar to that reported by Lai and Ramanath.[1,2] The making of the device begins with a double-sided polished Si wafer (1). Unlike processing of integrated circuits, where traditionally only one side of the wafer is patterned and etched, it is typical in MEMS to process on both sides.

Step (2) involves growing a thin silicon nitride film on both sides of the wafer. The film is grown by means of Plasma-Enhanced Chemical Vapor Deposition (PECVD). During the deposition, the substrate is held in a vertical position so that both sides have a silicon nitride film. Silicon nitride thin films grown by PECVD generally have less residual stress than do films grown by other methods.[3] This is beneficial for our purposes because the silicon nitride film will eventually form our membrane and it must be robust enough to sustain and support deposition of the metal heater. Silicon nitride films have been grown as thick as 0.3 microns and as thin as 200 Å.

Step (3) and (4) involves coating the front and backsides of the wafer with photoresist. The photoresist on the backside of the wafer is patterned using photolithography. The pattern will ultimately determine the window dimensions. Upon development (5), the patterned parts of the photoresist are removed.

Once the pattern is established on the backside of the wafer (6), Reactive-Ion-Etching (RIE) is used to remove the silicon nitride film. In step (7), wet KOH etching is used to remove the Si and leave a free-standing Si_3N_4 membrane. KOH etching is isotropic so the sides of the window are at an angle unlike RIE. KOH etching is used because for removing Si it is much faster than RIE. However, to etch through the whole silicon substrate requires several hours.

In step (8), a new coating of photoresist is applied. Again in step (9), the photoresist is patterned. This time, however, the pattern is reversed. That is, the exposed photoresist is removed, while the unexposed remains. This results in openings that define the final metallization boundaries.

Once the patterning is complete, the metal of choice (Ni, Pt, Au or Co) is deposited (10). The remaining photoresist also must be removed and so the whole wafer is placed in an acetone bath for liftoff of the metal (11). Upon drying, the calorimeter sensor is complete! Generally, an additional annealing step done in vacuum is conducted on the calorimeter before actual use.

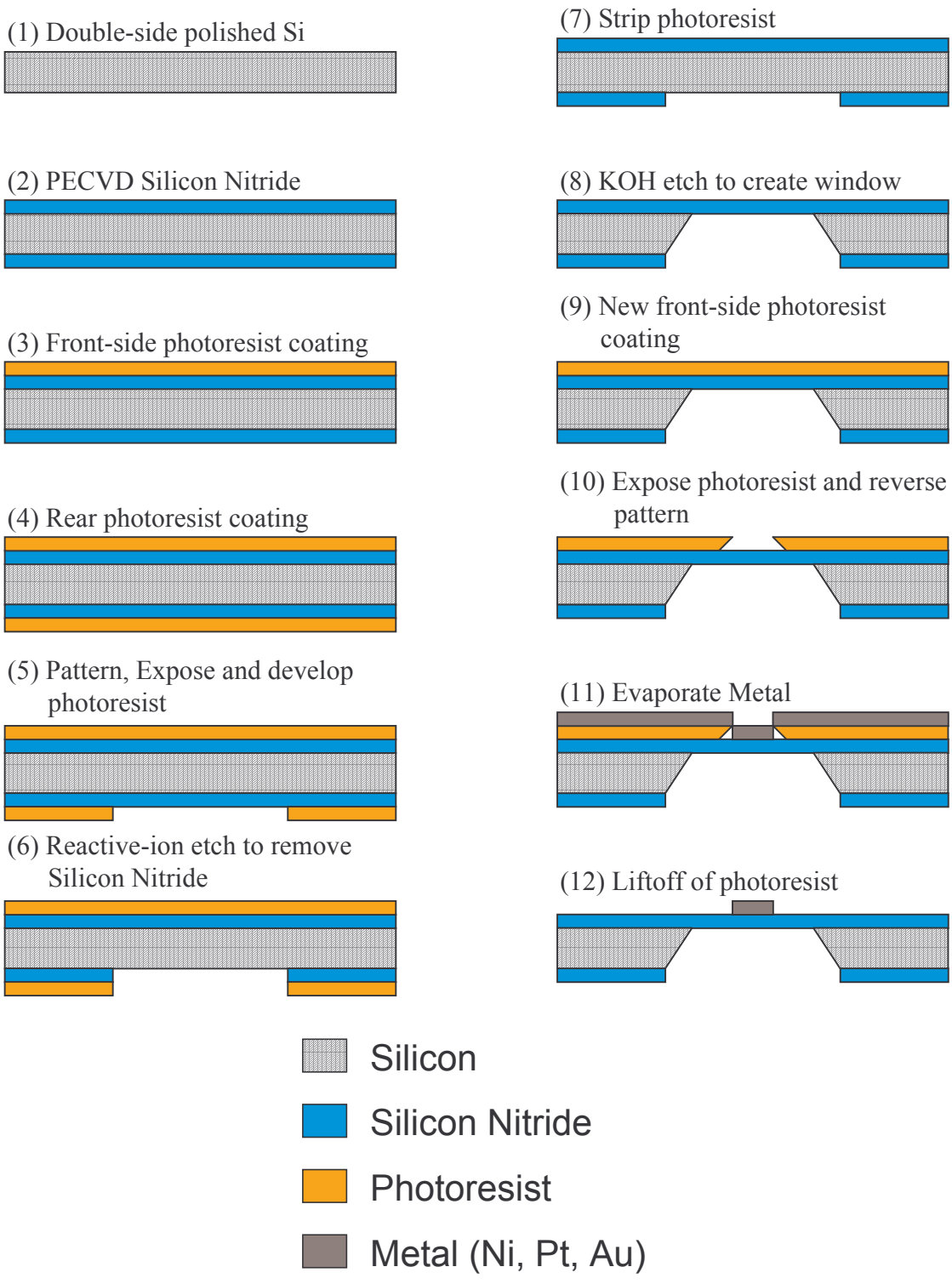

Figure 3.2. The processing steps involved in fabrication of the device. There are twelve basic steps that result in a metal heater/thermometer resting on top of a silicon nitride membrane.

III.3. Operation of the Nanocalorimeter

Nanocalorimetry relies on the MEMS calorimetric sensors. The planar and cross-sectional configurations of the nanocalorimeter are shown in Figure 3.3. The sensor consists of an extremely thin (30 nm) amorphous silicon nitride membrane (a-Si_3N_{4-x}) supported by a silicon frame.

On one side of the membrane, a patterned thin (50 nm) platinum strip (500 μm × 5 mm, ~70 Ω) is deposited, and is used simultaneously as a heater and resistive thermometer during the experiments. The material of interest is deposited on the silicon nitride side so that it rests above the heater/thermometer. Differential calorimetry is achieved by using two identical sensors in one setup — a sample sensor (with material) and reference sensor (with no material).

The calorimetric measurement is initiated by applying a synchronized DC electrical pulse (9 – 25 mA and 2 - 10 ms long) to each metal heater. The temperature of the sensors increases by Joule heating and typically reaches 200 °C at the end of the pulse. High heating rates ($2 \times 10^4 – 10^5$ °C/s) under high vacuum conditions (~10^{-6} torr), allow the measurements to approach adiabatic conditions. The current and voltage through the sensors are measured and used subsequently for power, resistance, and temperature calculations. The first pulse results in a significantly different endotherm peak in the case of the PE single crystal than the subsequent pulses. For this reason, the calorimetry data presented in this paper represents the first pulse separate from the subsequent pulses. For reduction of noise, over 100 pulses after the first pulse were conducted and averaged during each experiment.

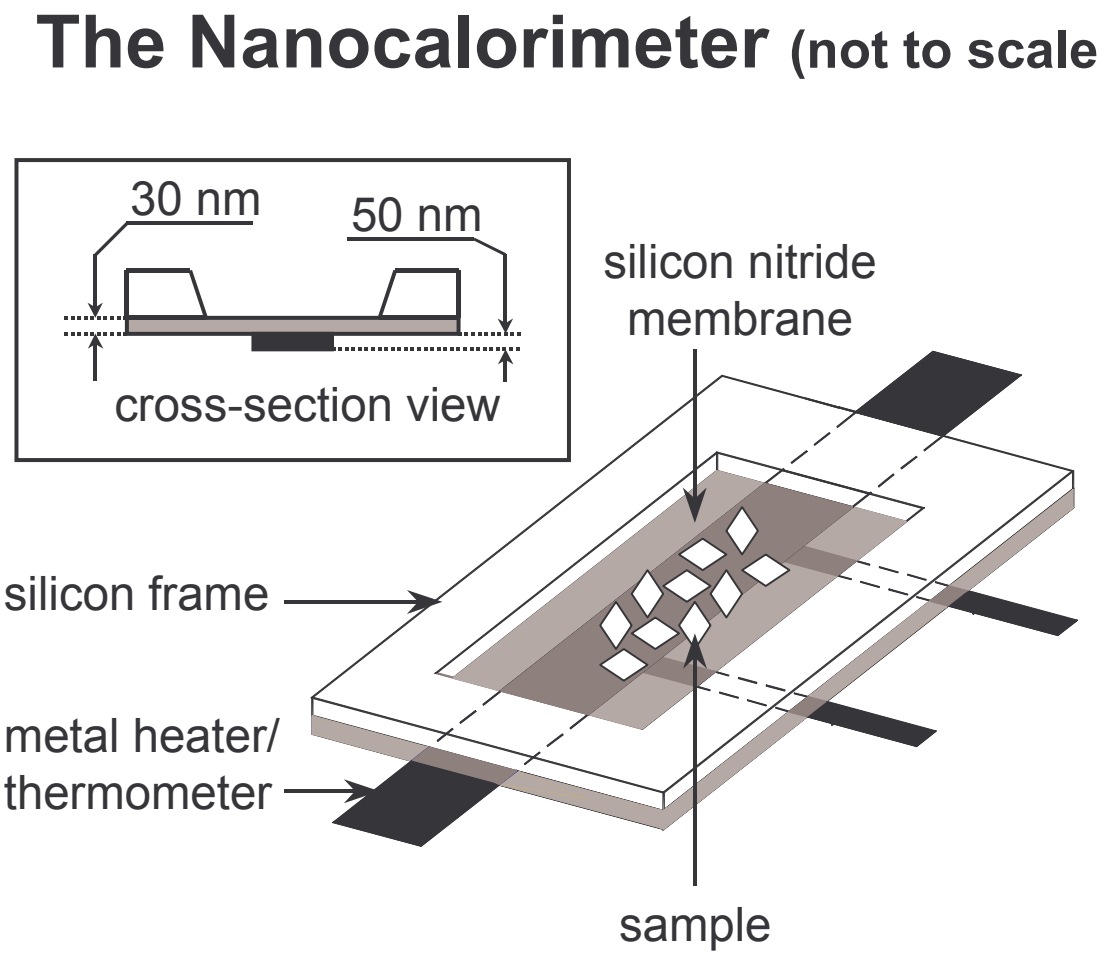

Figure 3.3. A schematic of the nanocalorimeter. The sample, polyethylene single crystals, is deposited on top of the heater area. Included is a cross-section view of the sensor. Relative dimensions have been exaggerated for clarity.

In the ideal case where the two sensors increase in temperature at exactly the same rate, the power required to melt the sample deposited on the sample calorimeter would simply be

$$P(t) = V_S I_S - V_R I_R \qquad (2)$$

where V and I denotes the voltages and currents through the sample and reference (indexes S and R, respectively) sensors, and t is time. The heat capacity would then be

$$C_P(T) = \frac{P(T(t))}{dT/dt}. \qquad (3)$$

However, our system deviates from the ideal case due to several conditions. An in depth discussion of the details of the data calculation to account for these non-ideal conditions may be found in Zhang et. al.[4] Calorimetric data are presented as a dependence of heat capacity, C_p, on temperature, T.

To conduct the annealing experiments, the power supply was modified to apply discrete, short, low-current pulses incrementally so that a controlled temperature ramp rate was possible. By careful adjustment of the temperature, abrupt stoppage in the ramp rate is possible and the system can be held at the desired annealing temperature for long or short times. Several parameters can be consequently controlled: time at anneal, ramp rate to annealing temperature, and annealing temperature.

III.4. Temperature Calibration

Before the experiment, both the reference and sample sensors are calibrated in a furnace using a calibrated thermocouple as the reference temperature probe. As a control experiment, indium was deposited, at a thickness where size-dependent melting does not occur[5], on the sensor and its melting temperature was recorded as another means of calibrating the sensor for accurate temperature measurement.

III.5. Polyethylene Single Crystal Growth

The source material used in the experiments was a high-density linear polyethylene with a density of 0.96 g/cm^3 and a melt index of 3.4 and was in the form of a blown film produced by Visking Co. in ca. 1960. To obtain single crystals, we prepared a 5 x 10^{-4} wt% solution by dissolving the polyethylene in xylene at 125 ^{o}C. The solution was quenched in an ice water bath and a self-seeding method followed.[6] The self-seeding method involves slowly heating the solution to a "seeding" temperature, 99 °C, to dissolve most of the crystals formed upon quenching and leaving only a small number of nuclei in solution. After the self-seeding, the solution was transferred to a beaker in an oil bath and the crystals were grown isothermally at 70 ± 2 ^{o}C for several hours. The resulting typical crystal has the form of a platelet that is nanometers thick and has lateral dimensions of microns.

To transfer the crystals onto the nanocalorimeter, the crystals were sprayed on by means of an airbrush unit. Care was taken to spray at a low velocity and for short times as to not damage the crystals in flight and insure the rapid evaporation of the solvent. After deposition of the sample, the calorimetric cells are pumped down to 10^{-6} torr in an evaporation chamber with a diffusion pump and calorimetric measurements are performed.

III.6. TEM

For electron microscopy, the crystals were deposited on a silicon nitride membrane (similar to the TDSC sensor but without the heater portion). No additional coating or staining was done on the crystals. Diffraction and bright field images were obtained for several crystals before and after calorimetric measurements. As expected[7],

the diffraction patterns lasted a very short time. The crystals were examined with a Phillips CM-12 TEM at 120 keV.

III.7. AFM

Because the sample size is so small, using a microbalance is not feasible to determine the mass. Thus mass was approximated from the volume as determined with a conventional optical microscope in conjunction with a Digital Instruments Nanoscope III atomic force microscope (AFM). From the optical microscope we obtained the number of crystals present on the sample sensor. From AFM imaging, we obtained the volume of individual crystals by determining the shape, lateral dimensions and thickness. The number of crystals multiplied by the volume of a typical crystal yields the total volume of material on the sensor. We followed the same method as Nakagawa and coworkers to obtain images with the AFM.[8] The samples were observed in contact mode with a V-shaped silicon nitride cantilever with an integrated pyramidal tip. The cantilever had a length of 200 μm and a spring constant of 0.12 N/m. The images were obtained in constant force mode with an applied force on the order of 10 nN. After image correction for image tilting and bowing, the lamella thickness was measured by section profile and depth analysis tools provided by Digital Instruments.

List of References

[1] Lai, S.L.; Ramanath, G.; Allen, L.H., Appl. Phys. Lett. 1995, 67, 1229.

[2] Lai, S.L.; Ramanath, G.; Allen, L.H., Appl. Phys. Lett. 1997, 70, 43.

[3] Ohring, M. In The Materials Science of Thin Films; Academic Press; San Diego, CA, 1992; p. 182.

[4] Zhang, M.; Efremov, M.Yu.; Schiettekatte, F.; Olson, E.A.; Kwan, A.T.; Lai, S.L.; Wisleder, T.; Greene, J.; Allen, L.H., Phys. Rev. B 2000, 62, 10548.

[5] Efremov, M. Y.; Schiettekatte, F.; Zhang, M.; Olson, E. A.; Kwan, A. T.; Berry, R. S.; Allen, L. H., Phys. Rev. Lett. 2000, 85, 3560.

[6] Blundell, D. J.; Keller, A. J. Polym. Sci., B, 1968, 6, 433.

[7] Geil, P. H. In Polymer Single Crystals; John Wiley and Sons: New York, 1963; p 24.

[8] Nakagawa, Y.; Hayashi, H.; Takahagi, H.; Soeda, F.; Ishitani, A.; Toda, A.; Miyaji, H., Jpn. J. Appl .Phys. 1994, 33, 3771.

IV. RESULTS AND DISCUSSION

IV.1. Ni Foil Calorimetry

The Ni foil calorimeter aimed to demonstrate that calorimetric measurements could be made with a metal resistor that acts as both the heater and thermometer. To this end, the experiments were successful. First, measurements were taken to obtain the heat capacity of the Ni in the Ni foil calorimeter by conducting pulses without any sample on the heater. Using a conventional DSC, the heat capacity of Ni (taken from the same foil as the Ni foil calorimeter is constructed of) was also determined. A comparison of the results can be found in Figure 4.1. Also shown in the figure is the heat capacity from the JANAF tables. It is evident from the data that the DSC and the Ni foil calorimeter obtained measurements that agreed with one another. Both methods obtained slightly different values (< 15%) from the JANAF values. The difference is most likely due to the makeup of nickel used in the experiment. Nevertheless, this indicates that calorimetric measurements can be conducted using a metal heater/thermometer with comparable results to DSC.

Figure 4.2 shows the results of the experiments with a polyethylene film as the sample as well as DSC measurements on the same film. The DSC measurement was taken with a scan rate of 10 ^{o}C/min (0.16 ^{o}C/sec). The Ni-foil calorimeter measurements were taken with scan rates from 40 to 1500 °C/s. At low heating rates, our data indicates a melting point that agrees with data obtained by DSC (within 5 ^{o}C). At higher heating rates, our data indicates increasing melting points (shifts of +10 °C). I believe this is due to a thermal lag across the 24 μm polyethylene film thickness.

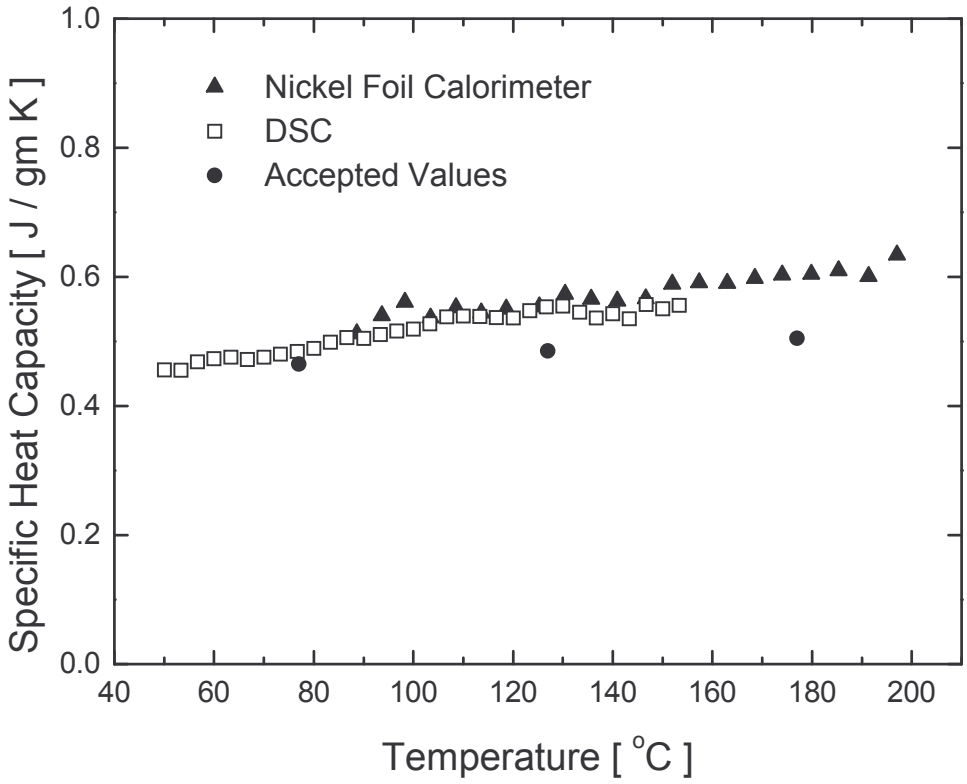

Figure 4.1. A comparison of DSC, Ni foil calorimeter, and accepted values is shown. Measurements made by DSC and the Ni foil calorimeter agree well with each other and accepted values. The accepted values were obtained by JANAF.[1]

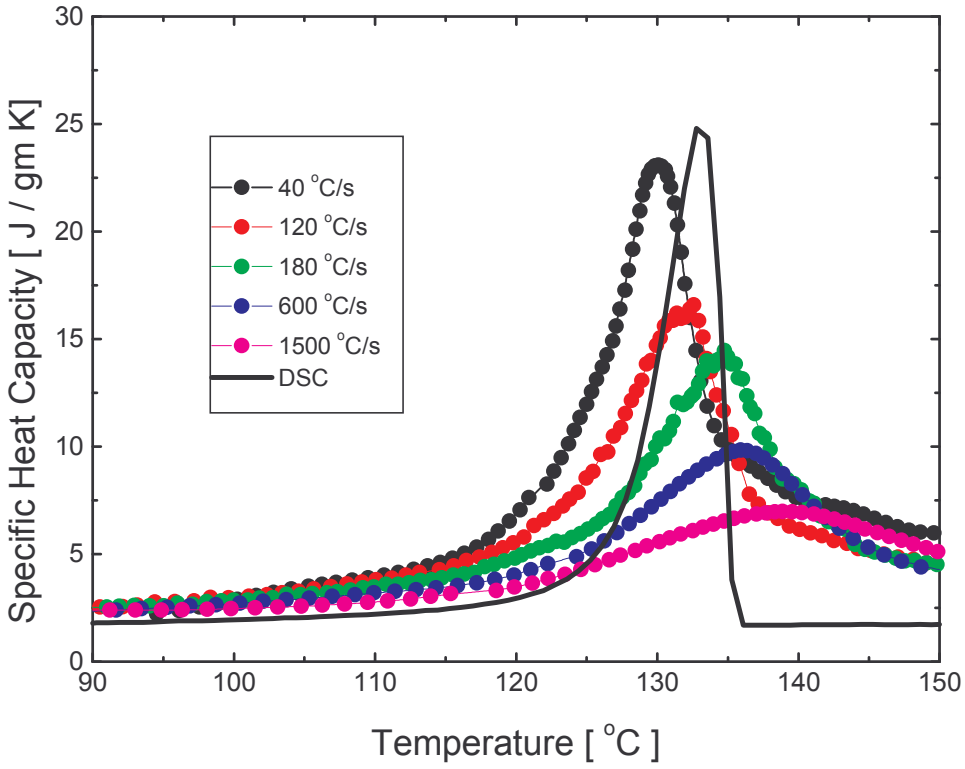

Figure 4.2. Comparison of DSC and Ni foil calorimeter measurements for the melting of a polyethylene film. At faster heating rates, as measured by the Ni foil calorimeter, the melting endotherm broadens and shifts to higher temperatures indicating thermal lag in the system.

Furthermore, the difference can also be attributed to poor calibration of the Ni foil as a thermometer, since only a hot plate was used. The heat of fusion of melting however remains in good agreement (within 20%) with that obtained by DSC regardless of heating rate. Again, this demonstrates that calorimetric measurements are possible using this method. By scaling down the system the sample, using faster scan rates during the experiment, and performing more accurate temperature calibration, more sensitive and reliable calorimetric measurements are possible.

IV.2. Structural Characterization

Figure 4.3 shows an AFM image of a typical polyethylene single crystal studied in our experiments. Our images of the single crystals were similar to those obtained by Kawaguchi and coworkers[2] with similarly grown crystals. The majority of crystals were lozenge-shaped with a length of 20 μm, a width of 13 μm, and a thickness of 12 ± 1 nm. Some of the lozenge crystals, however, had spiral growths. Other crystals were star-shaped and had multiple layers. No matter what the crystal shape, AFM measurements yielded consistent lamella thicknesses. Several crystals of each shape were imaged and analyzed so that a volume could be assigned to each shape type. Hence, each shape type—lozenge-shaped, lozenge-shaped with spiral growths, and star-shaped—were imaged and counted. In this way, we determined the total volume of sample detected by the calorimeter.

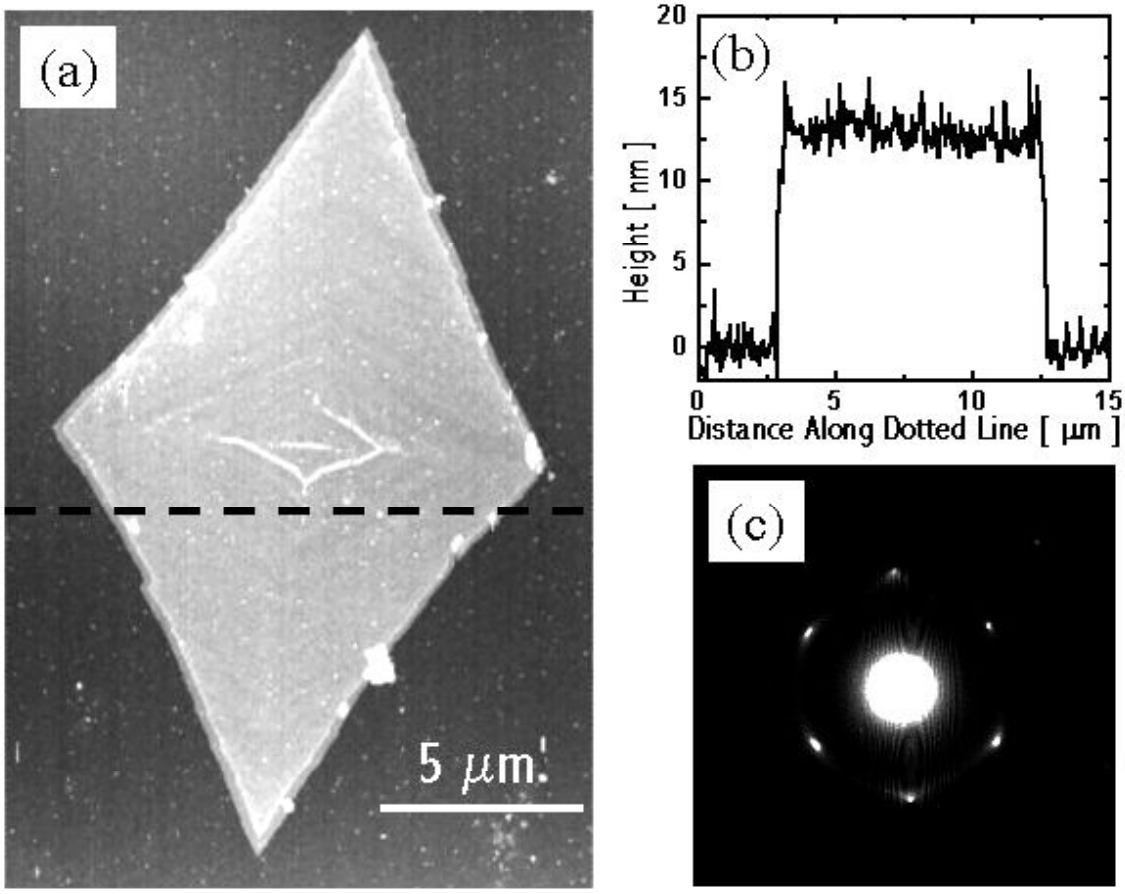

Figure 4.3. (a) AFM micrograph of a typical 20 μm × 13 μm × 12 nm single crystal. The pleats near the center of the crystal are a result of the original tent-shaped crystal collapsing on the flat silicon nitride surface. (b) The section profile of the crystal. The x-axis of the profile corresponds to the dotted line in (a). (c) A diffraction pattern obtained by TEM of a similar crystal.

To arrive at the sample mass, we multiplied the total volume of crystals by the density of the material used for fabricating the original film (0.96 g/cm^3), assuming the density of the single crystals was equal. In addition, calculating the sample mass by means of volume is also complicated by the by error associated with volume calculation and counting. These errors can contribute an additional 15% uncertainty. By taking enough data at varying amounts of crystals, the sample mass calculated in this manner provides a means of verifying our calorimetric measurements since the thermal properties of heat capacity and heat of fusion are extensive—they scale with amount.

IV.3. Calorimetric Measurements

A control experiment was performed in which In was deposited on the non-heater side and PE was sprayed on the heater side. As shown in Figure 4.4, the melting peak of In is determined to be at about 156 ^{o}C according to our measurements. Though the peak is broader than expected, this indicates that the method of temperature is adequate to presuppose an error in temperature measurements of no more than ± 3 ^{o}C.

Figure 4.5a shows the normalized results for a 30 crystal experiment. Also shown is the specific heat capacity of the bulk material (as obtained with a conventional DSC) for comparison. The endotherm from the as-deposited scan indicates the melting temperature of our single crystal polyethylene is 123 ± 2 °C. This value is about nine degrees less than the bulk. Previous work has also determined the melting temperature, albeit not by calorimetry, of polyethylene single crystals grown from solution. Table 4.1 summarizes their results for comparison with our work. Our work agrees well with optical microscopy experiments on similarly grown crystals conducted by Hellmuth and Wunderlich.[3] Their experiments consisted of several trials of monitoring changes in

appearance during heating with an optical interference microscope. Their samples were growth spirals of single crystal polyethylene consisting of 100 – 200 lamellae with a total thickness of 2000 nm, grown from a dilute solution of toluene. At heating rates of 2- 33 ^{o}C/s, the melting point was 121 ± 2 ^{o}C. Our melting temperature also agrees with results of Alamo and Mandelkern.[4] Their experiments consisted of studying the crystallite thickness distribution as determined by Raman LAM spectroscopy of a sample annealed at different temperatures (112 – 150 ^{o}C). They concluded that the melting of powders of solution grown polyethylene (M_w = 166,000; M_w/M_n = 1.11) single crystals, with a thickness of ~13 nm, occurs below 125 ^{o}C.

Another important characteristic of the single crystals, apparent in Figure 4.5a, is the difference in the endotherm peak of the first pulse and the subsequent pulses. There is a 50% reduction in heat of fusion from the as-deposited crystals to subsequent quenched crystals. Also, there is a shift in the peak of seven degrees. This may be attributed to the fast cooling, essentially quenching, of the polyethylene crystals from a molten state to a solid state. The cooling occurs within several milliseconds. The phenomenon has also been reported by Grubb and coworkers.[5] During their experiments using real time SAXS studies with annealing of polyethylene single crystals, they noticed that heating occurred much slower on the first ramp than the subsequent ramp. They attributed this to the "greater amount of endothermic reorganization" that occurs on the first heating. So it is suspected that after the initial melting, there is a loss of crystallinity upon cooling. This was confirmed using TEM. Figure 4.3c is a diffraction pattern obtained by TEM before any heating. After heating no diffraction pattern was observed.

	Source Material	Lamella Thickness	Method of Analysis	Melting Temperature	Reference
This Work	Density of 0.96 g/cm^3; Melt Index of 3.4	12 ± 1 nm	Thin Film Differential Scanning Calorimetry	123 ± 2 ^{o}C	
Hellmuth and Wunderlich	M_w = 80,000	10-20 nm	Optical Interference Microscopy	121 ± 2 ^{o}C	4
Alamo and Mandelkern	M_w = 166,000	~13 nm	Annealing followed by Raman LAM Spectroscopy	Below 125 ^{o}C	5

Table 4.1. Comparison of this work with previous experiments. Despite the differences in starting material, the melting temperature of the three experiments agree with one another.

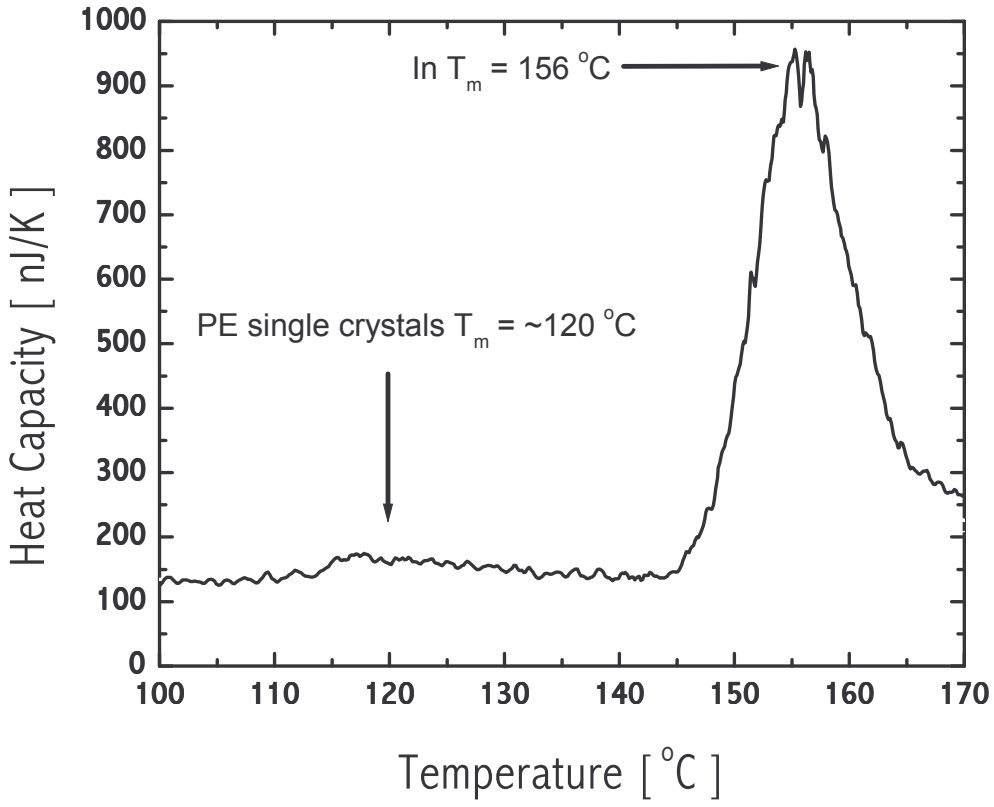

Figure 4.4. The heat capacity data for the control experiment which had both In and PE deposited on the sensor. The data indicates that the temperature calibration method used in the experiments with PE single crystals is adequate and yields a reasonable boundary of error for our purposes.

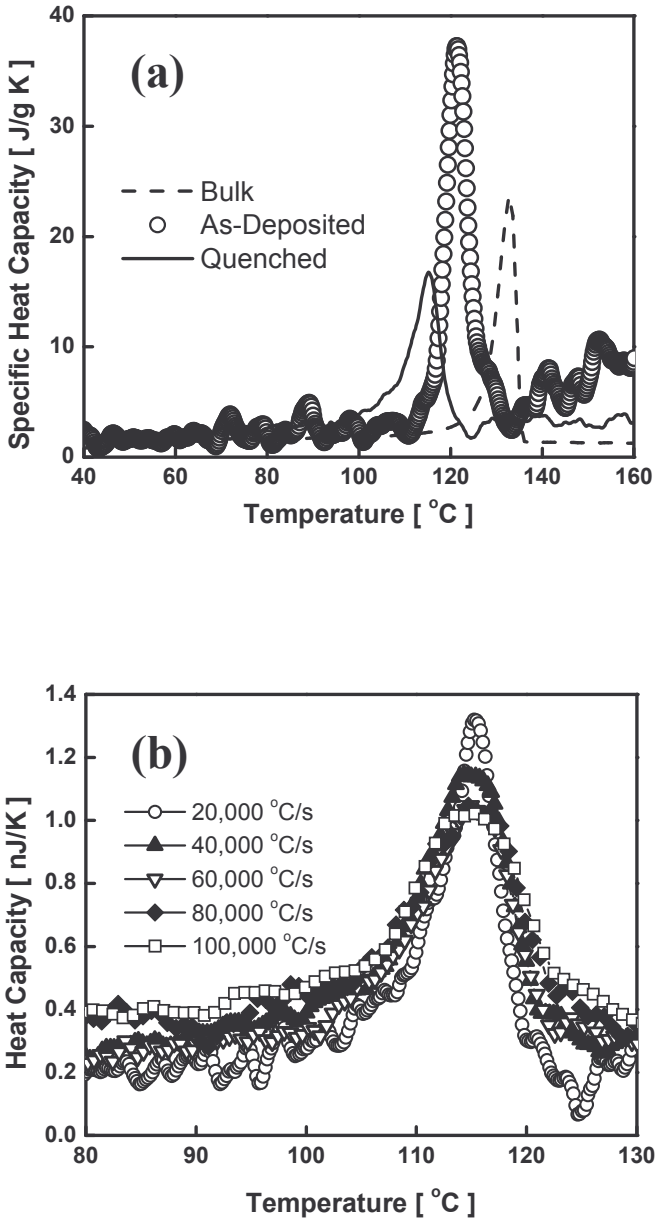

Figure 4.5. (a) The specific heat capacity for the source material, from the first pulse, and the subsequent pulses for 30 crystals at a heating rate of 20,000 °C/s is shown. For clarity, the as-deposited and quenched scans were smoothed with a 15-point adjacent averaging. (b) Also shown is the endotherm of the quenched scans at varying heating rates. Its position and shape does not change significantly with heating rate. For purposes of clarity, the data has undergone a 5-point adjacent average smoothening.

It should be noted that we obtained consistent values for ΔH_f (± 15 %) over a wide range of heating rates. Figure 4.5b shows the endotherm for the 30 crystal experiment at heating rates from 20,000 to 100,000 ^{o}C/s. In the subsequent pulses, the peak of the endotherm remains constant at about 116 ^{o}C as the rate increased. The full width at half maximum of the peak increases from six to ten degrees. This may be due to the limitations of the instrument; at higher heating rates the temperature resolution is not as good as at low heating rates and thus during calculations to arrive at an endotherm a broader peak may arise. We do not believe either superheating or thermal lag is occurring because though the peak may widen, it does not shift to higher temperatures.

The latent heat of melting was calculated by integrating the area under the heat capacity peak of the first scan. Figure 4.6 shows the heat of fusion of 25 to 2000 single crystals as a function of mass calculated from volume for the given amount of crystals. Also depicted is the heat of fusion (solid and dashed line) assuming the same specific latent heat of melting of the bulk (as measured by conventional DSC). Taking the slope of the raw data in Figure 4.6 yields a specific latent heat of melting for polyethylene single crystals of 198 ± 10 J/gm, which is 40 % greater than the bulk value, 140 J/gm.

The measured heat capacity (between 40 and 60 ^{o}C) also scales in relation to the sample mass (Figure 4.7). The specific heat capacity calculated in the same manner as the specific latent heat of melting (taking the slope of the measured heat capacity of the isolated single crystals with respect to mass) yields a specific heat capacity of 2.1 ± 0.3 J/gm K. This value is within 25 % of the bulk value, 1.7 J/gm K (as determined by DSC).

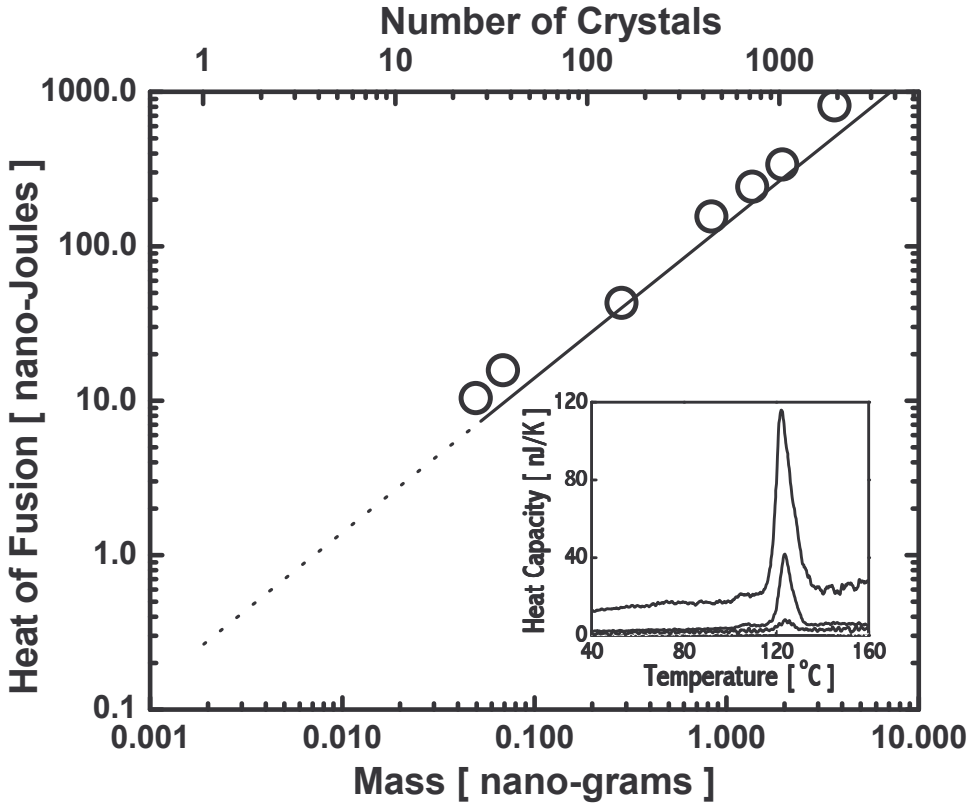

Figure 4.6. Heat of fusion of 25 – 2000 polyethylene single crystals. The bottom axis indicates the mass as determined by volume calculations. The top axis indicates the number of 20 μm × 13 μm × 12 nm polyethylene single crystals. The solid and dashed lines indicate the expected heat of fusion using the bulk value. The inset graph shows the heat capacity of 120, 680, and 2000 single polyethyelene single crystals.

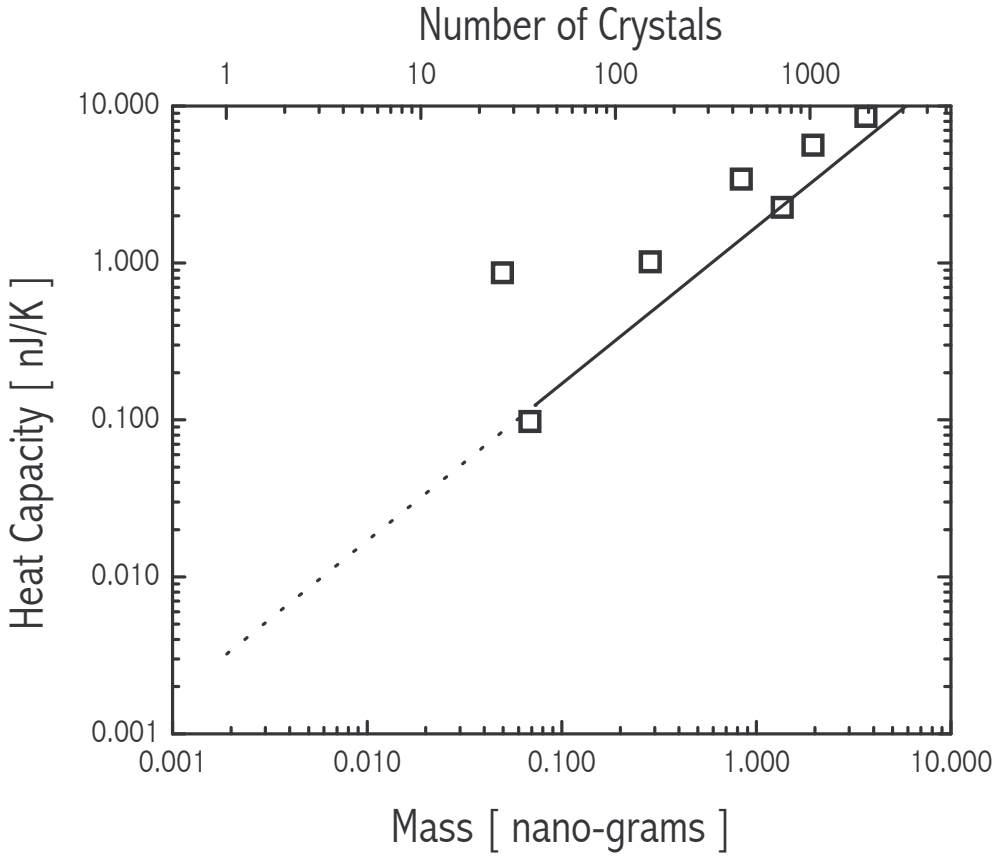

Figure 4.7. Average heat capacity of 25 – 2000 polyethylene single crystals. The bottom axis indicates the mass as determined by volume calculations. The top axis indicates the number of 20 μm × 13 μm × 12 nm polyethylene single crystals. The solid and dashed lines indicate the expected heat capacity using the bulk value.

IV.4. Limitations of Measurements

At a lower numbers of crystals, the effect of handling during crystal deposition, are more pronounced. Addition of material that does not undergo a transformation near that of polyethylene would contribute to the heat capacity but not to the heat of fusion. Thus at these lower amounts, the data for heat capacity deviates from what is expected, but the heat of fusion appears more consistent.

Obtaining calorimetric measurements involves three steps as described in the earlier. First, the calorimeter is placed in the vacuum chamber and the pressure is reduced to $\sim 10^{-6}$ torr and drift and baseline measurements are taken. The drift measurements involve pulsing the calorimeter several hundreds of times, to remove any drift in the signal or at least until drift is minimal. Baseline measurements are needed for the correction factors used in the actual data analysis. Once these measurements are taken, the second step involves opening the chamber and spraying the PE crystals onto the calorimeter. The last step involves pumping back down and performing the measurements with the sample, the PE crystals, on the sample calorimeter. The second step is a crucial step because it introduces several uncertainties that can affect calorimetric measurements.

The second step requires physical removal of the sample calorimeter from the chamber. The consequences of removing the calorimeter can include: movement of the mechanical contacts to the voltage and current metal pads on the sensor or stray particles landing on the heater. The first consequence can result in a slight change in the current or voltage measured in subsequent measurements. With a change, the baseline measurements are rendered almost useless. The second consequence can result in additional material being measured during calorimetric measurements. Ideally, only PE

crystals would be measured. With stray particles, the heat capacity measured will not be solely due to the PE crystals but instead be due to the crystals and the stray particles.

Spraying of the crystals in an open atmosphere can also possibly introduce stray particles onto the calorimeter. The xylene solvent can leave residue besides PE crystals on the calorimeter. The same concern of additional material besides the PE crystals affecting calorimetric measurements therefore also exists due to actual spraying itself.

Therefore it was important to gain an idea if removing the calorimeter and spraying of solvent really do affect measurements. Figure 4.8 shows the results of two sets of control experiments. The first experiment involved following the usual three steps but instead of spraying crystals onto the calorimeter in the second step, the calorimeter was removed from the chamber and held in atmospheric conditions for about five minutes (about the same amount of time needed to do the actual spraying). The second experiment also involved following the three steps but instead of spraying crystals onto the calorimeter, 200 sprays of only solvent were conducted. 200 is the same number of sprays done for the 1000 crystal experiment. Both control experiments indicate that the second step of sample deposition can directly affect the accuracy of calorimetric measurements.

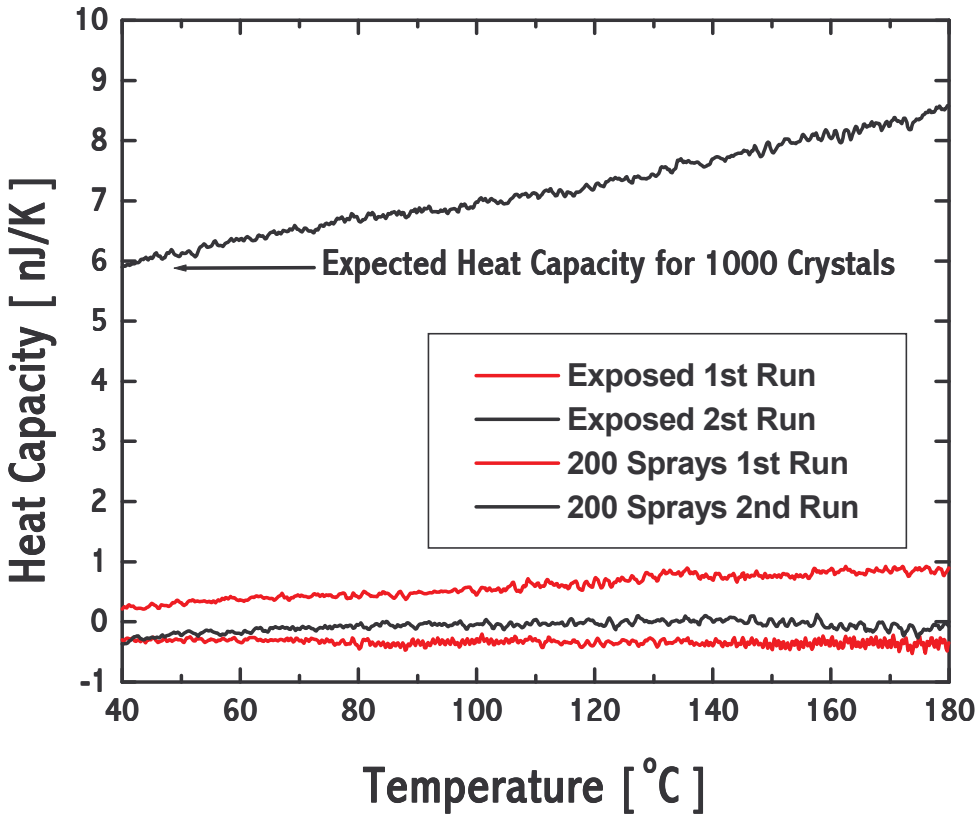

Figure 4.8. The results of two control experiments. Merely exposing the calorimeter to atmospheric conditions before calorimetric measurements can result in unreliable values for heat capacity. Also, the solvent can introduce anomalies in calorimetric measurements.

Taking the average heat capacity between 40 and 60 ^{o}C can result in a heat capacity of -0.2 nJ/K. Such a variation is equivalent to one hundred crystals. Furthermore, taking the average heat capacity between 40 and 60 ^{o}C for the 200 sprays experiment can result in a value of 6 nJ/K, which is equivalent to a thousand crystals. These two experiments are not an exhaustive study of the contributions of the uncertainty due to sensor handling or sample deposition but they do demonstrate that they can affect measurements. Therefore, as the technique stands, it is very difficult to obtain trustworthy heat capacity measurements at low amounts of crystals.

IV.5. Surface Effects

One concern while performing calorimetric measurements was the effect of the surface on the crystal properties. Traditionally, the sample in the early experiments, with the nanocalorimeter, was deposited on the non-heater (silicon nitride) side as depicted in Figure 3.3. The basic reason behind this choice to deposit on the non-heater side is that the early experiments studied metals (Sn, In) and the presence of the silicon nitride membrane ensured electrical isolation of the sample from the metal heater.[6] With polyethylene, because it is non-conductive, performing experiments with the crystals deposited on the heater is possible.

However, the nanocalorimeter rests heater side up due to the construction of the device holder. Hence, it is more feasible to spray the crystals on the heater rather than onto the other side. Furthermore, because the nanocalorimeter is essentially a narrow and small cavity on the non-heater side, imaging with an AFM is more difficult if the sample were deposited there. The AFM tip holder grinding into the Si frame is a real concern if the tip is not properly positioned. Consequently, the first experiments with polyethylene involved deposition of the crystals on the heater.

After obtaining AFM images of the several crystals on the nanocalorimeter after the first two polyethylene experiments were performed, it was noticed that the crystals on the heater had a different morphology than the crystals near the heater (on the membrane but close enough to be heated). A good example of the difference in morphology is shown in Figure 4.9a. The AFM micrograph shown has a crystal partially on the heater and partially on the membrane. On the heater, the crystal is continuous like the as-deposited crystal of Figure 4.3a, but it is not as smooth and appears to have several ridges. Off of the heater, the crystal is discontinuous and appears to ball up.

Two possible issues might cause the difference in morphology. First is the issue of the surface. The crystal may rather wet the metal heater and is abject to wetting the silicon nitride. So after heating, the crystals on the metal will wet the heater but the crystals on the membrane ball up instead. Second is the temperature gradient from the heater edge to the silicon nitride. It is apparent that crystals, which are more than 50 μm away from the heater's edge, have the same morphology as as-deposited crystals. It is assumed that they do not undergo melting during the experiments. Thus the 50 μm distance between the heater's edge and the region where no melting occurs must have some thermal gradient during the experiment. It may be that the thermal gradient results in crystals near the heater's edge to be heated but never to their melting temperature. Thus they are essentially annealed. It has been observed under AFM that similar polyethylene single crystals annealed to 120 ^{o}C developed holes[7] in a similar way to the right-hand portion of the crystal in the AFM micrograph of Figure 4.9a.

It is difficult to conduct an in depth study of the thermal gradient but it was more feasible to probe the surface effects by depositing the crystals on the non-heater side. If

by depositing the crystals on the non-heater side we observe differences in the calorimetric data or morphology, then it suggests that the surface does affect the crystal structure. What was found, however, was not entirely conclusive as shown in Figure 4.10b. Deposition of the crystals on the non-heater side did not result in a significant change in the caloric curves. The slight differences are not beyond reasonable experimental variations. The morphology as observed by the AFM (with some ingenuity in the tip positioning), however, appeared different than the heater-side case. The micrograph of Figure 4.9b shows a crystal in the same orientation as in Figure 4.9a. The left-hand portion of the crystal is above the heater but the right-hand portion is not. The left-hand portion is more continuous than the right-hand portion but neither portion has the globular morphology of the right-hand portion of the heater-side crystal. It is apparent, however, that the portion above the heater is not identical to the portion in Figure 4.9a on top of the heater. The non-heater side crystal still appears to not wet the surface.

It remains however, that the crystal on the heater side after calorimetric experiments differs from the crystal on the non-heater side but the calorimetric data is not affected. The data suggests that the different surfaces affects the morphology but does not affect the calorimetry. Furthermore, the temperature also affects the morphology. A greater understanding of the phenomenon would be had if different surfaces were used besides Pt and silicon nitride, rigorous modeling of the thermal gradient near the heater edge were performed, or direct characterization of the thermal gradient were conducted.

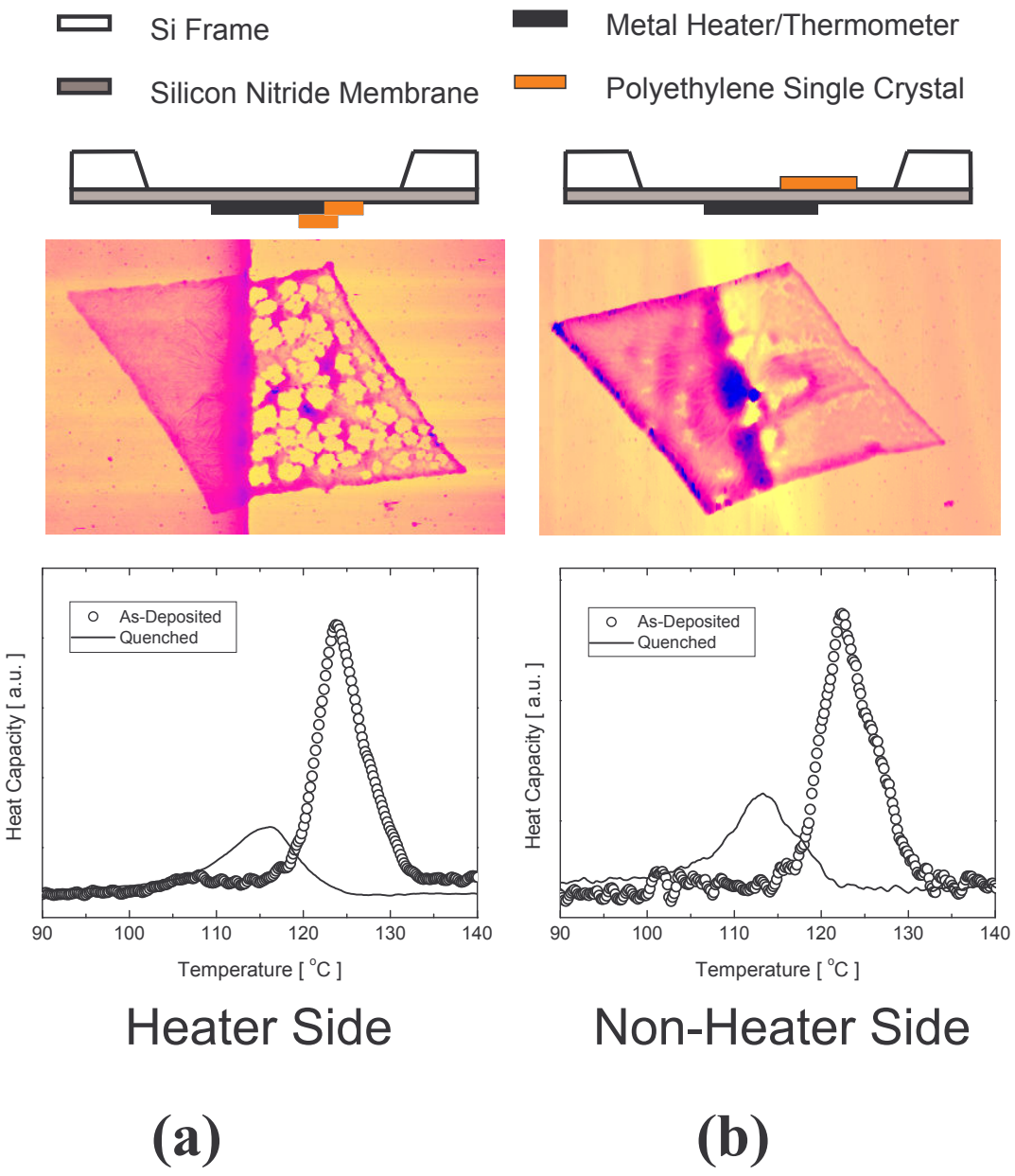

Figure 4.9. AFM micrographs of crystals that are partially on top of the heater and partially on the membrane. (a) The crystal lies on the heater side. The right half lies completely on the membrane while the left half lies on the metal heater. (b) The whole crystal is on the membrane side but the left half is above the heater whereas the right half is above only the membrane. Schematic representations are shown above.

IV.6. Annealing Effects

Thus far, we have been able to observe the effects of annealing of the quenched crystals obtained after the first pulse. Two sets of experiments were conducted on the same set of PE crystals. How the annealing temperature and the length of time at anneal affects the melting of the crystals was of prime interest. In the first set of experiments, the quenched crystals were annealed at different temperatures for one second. Figure 4.10 shows that the one second annealing did not yield an endotherm with the same area under the peak or peak position as the first pulse endotherm when the quenched crystals were annealed at different temperatures. However, we did observe a significant change in heat of fusion (increase of over 50%) and peak position (increase of up to 15 ^{o}C) from that of the unannealed quenched crystals by annealing at different temperatures. Furthermore, the systems always reverted back to the endotherm of the quenched state after any pulsing.

In the second set of experiments, we annealed the crystals at 123 ^{o}C for one second, two minutes, ten minutes, and 30 minutes. As shown in Figure 4.11, at longer times, the peak shifts to higher temperatures but the heat of fusion remains about the same. Upon quenching another one second anneal at 123 ^{o}C was conducted and the caloric curve agreed well with the first one second anneal at 123 ^{o}C. In future work, we plan to conduct annealing on the as-deposited crystals and conduct more in-depth structural studies in conjunction with calorimetry.

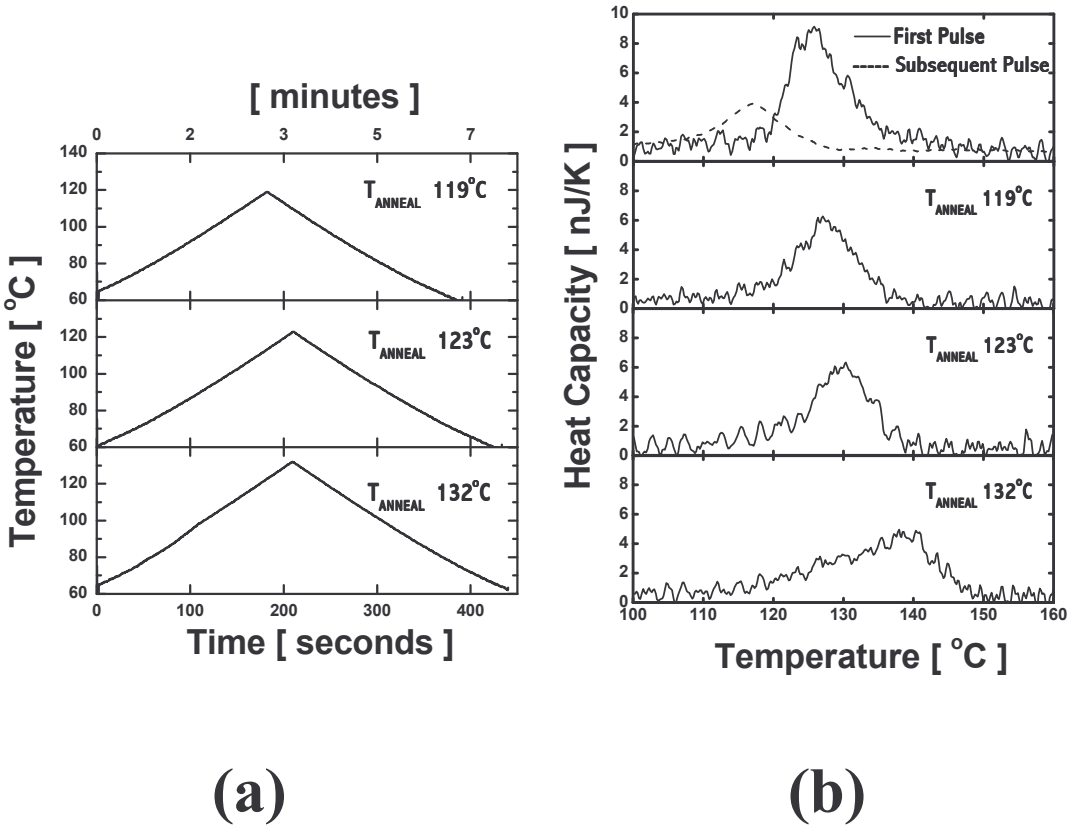

Figure 4.10. (a) The annealing scheme employed for each caloric curve. The same set of crystals was used for each trial. (b) The endotherm shifts to higher temperature upon annealing. However, the heat of fusion never reaches that of the first pulse. All anneals were conducted on the quenched crystals. After any calorimetry, the caloric curve returned to that of the quenched crystals (subsequent pulse).

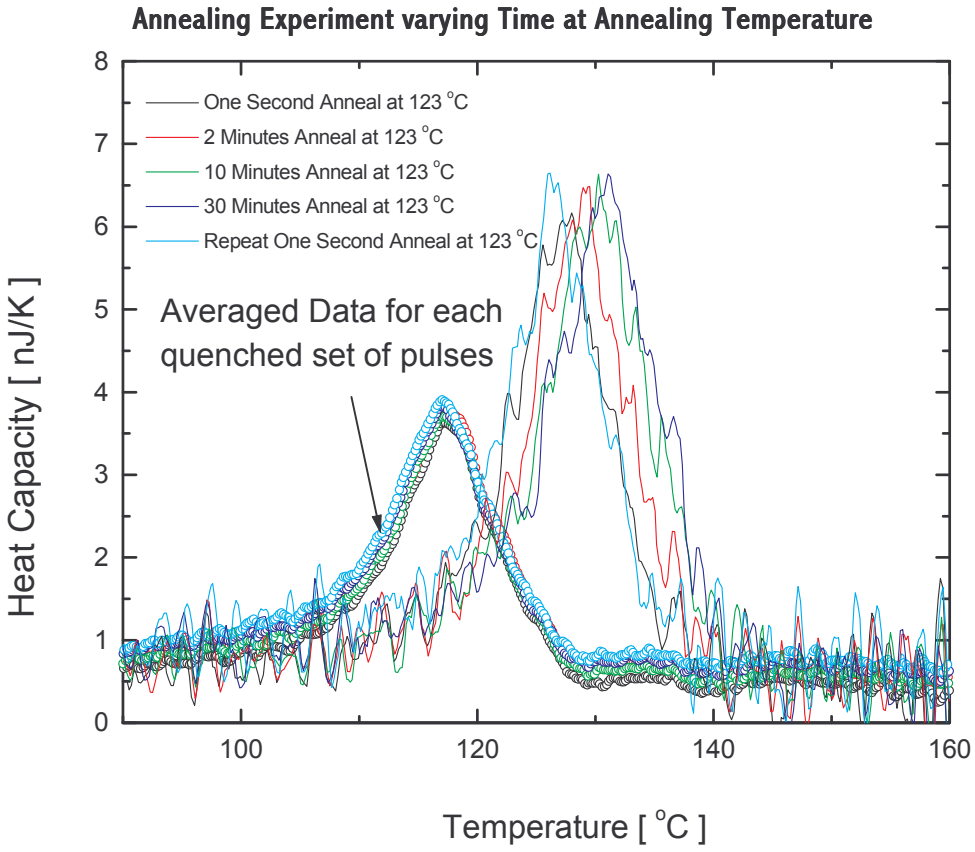

Figure 4.11. The same set of crystals was used for each trial. The endotherm shifts to higher temperature upon annealing at longer times. However, the heat of fusion never reaches that of the first pulse. All anneals were conducted on the quenched crystals. After any calorimetry, the caloric curve returned to that of the quenched crystals (subsequent pulse).

List of References

[1] JANAF Thermochemical Tables, (Washington D.C. 1966)

[2] Kawaguchi, A.; Ichida, T.; Murakami, S.; Katayama, K., Colloid. Polym. Sci. 1984, 262, 597.

[3] Hellmuth E.; Wunderlich, B., J. Appl. Phys. 1965, 36, 3039.

[4] Alamo R.; Mandelkern L., J. Polym. Sci. Part B: Polym. Phys. 1986, 24, 2087.

[5] Grubb, D.T.; Liu, J. J-H.; Caffrey, M.; Bilderback, D. H., J. Polym. Sci. Polym. Phys. 1984, 22, 367.

[6] Allen, L. H.; Lai, S. L., Microscale Thermophysical Engineering, 1998, 2, 11.

[7] Kajiyama, T.; Tanaka, K.; Ge, S-R.; Takahara A., Prog. Surf. Sci. 1996, 52, 1.

V. FUTURE WORK

The method in its current state, though robust and producing good measurements can be enhanced. With improved electronics in the data acquisition system (which is currently underway) that allow for better consistency in measurements and easier data processing, calorimetric measurements will become more repeatable, accurate, and feasible. In addition, a new design of the nanocalorimeter can also have benefits. The lowest amount of polyethylene detected was 25 crystals. This is pushing the limits of the nanocalorimeter in its present form. The surface coverage for 25 crystals on the present sensor area is less than 0.1%. By decreasing the sensor area, the sensitivity should be increased to allow the detection of the melting of a single crystal. This has strong implications for the world of polymer science. It may then be possible to probe the properties of individual crystals as opposed to merely the average of an aggregate.

Based upon this preliminary work, there are several endeavors to pursue in polymer science. In particular, the study of melting of PE single crystals at different thicknesses, the study of melting of PE single crystals after annealing, and the study of hexagonal PE single crystals are possible venues. In addition to the study of PE single crystals work on other polymers would be of great interest. There has been great interest in the polymer community concerning the glass transition of polystyrene (PS) thin films.

It has been suggested that PE single crystals undergo melting point depression with decreasing lamella thickness.[1] It is possible to grow PE single crystals at different thicknesses with good control of the crystallization temperature. It has been found that the lamella thickness of PE single crystals decrease with decreasing crystallization temperature.[2] A good oil or water bath is required to maintain a constant crystallization

temperature (± 0.5 ^{o}C) to obtain uniform lamella thickness for the crystals. Unfortunately, our group does not have this capability and we could not control the lamella thickness to observe a strong visible relationship between melting temperature and lamella thickness. With better equipment it is possible to control the lamella thickness and study the melting point of PE single crystals with different thicknesses.

As previously mentioned, the work presented in this thesis included only annealing experiments on quenched PE single crystals. It would be interesting to observe the changes in melting point and heat of fusion resulting from annealing as-deposited PE crystals. Such experiments would require annealing the as-deposited crystals at different temperatures (and possibly for different times) and then performing calorimetric measurements. AFM (for thickness measurements) and TEM (diffraction) characterization would contribute to these experiments as well. The results of the experiments would lend much to the discussion of how the crystals behave under thermal cycling that has been of considerable debate in the polymer world.[3]

Another worthy endeavor to pursue using the nanocalorimeter would involve comparing the thermal properties of hexagon-shaped PE single crystals to lozenge-shaped PE single crystals. Hexagon-shaped PE crystals mare grown from an octane solution (at crystallization temperatures of 110 – 116 ^{o}C) and are composed of {110} and {100} growth sectors. The lozenge-shaped PE crystals are grown in xylene at lower crystallization temperatures and are composed of only the {110} sectors. It is observed that the hexagon crystals have a thickness difference in the different sectors because the fold direction in the single crystals is thought to be along the growth face in each sector.[4] An AFM micrograph is shown in Figure 5.1a.

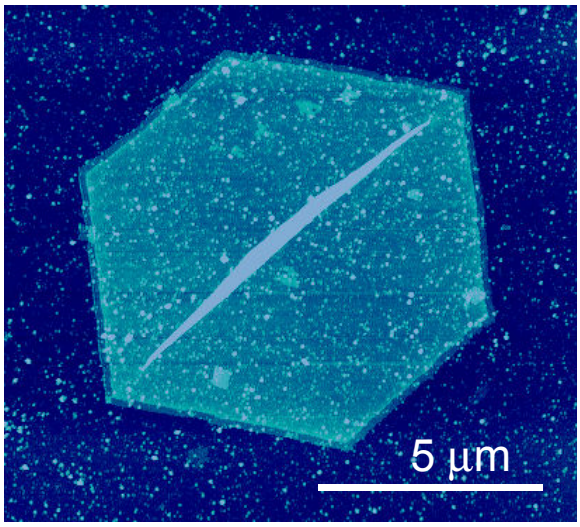

(a)

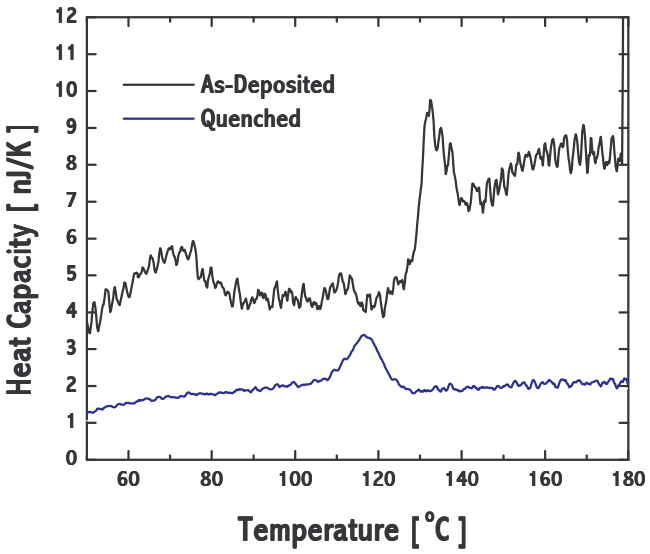

(b)

Figure 5.1. (a) An AFM micrograph of a hexagon-shaped PE single crystal. The crystal consists of four {110} sectors and two {100} sectors that are faintly visible in the slight contrast near the center. (b) Heat capacity of hexagon PE single crystals for the as-deposited and quenched crystals.

Because the hexagon crystals have sectors with two different orientations, it may very well be possible that two melting endotherms will be observed in the calorimetric measurements. One experiment has been conducted thus far. The results of the experiment are shown in Figure 5.1b. Shown are the data for the as-deposited and the quenched crystals. The as-deposited caloric curve is actually the first scan in a set of 110 scans. The quenched caloric curve is the average of the 10^{th} to 110^{th} scans. The second to ninth scan, unfortunately, were not recorded during the experiment due to poor foresight in the experimental design. During the measurement, however, it was observed that the second to ninth scan resulted in a gradual change from the as-deposited case to the quenched case. After the 10^{th} scan, little change was observed in the signal. No similar behavior was observed with the lozenge-shaped PE single crystals. With the lozenge-shaped PE single crystals, only the very first scan resulted in a different caloric curve. Unfortunately, time did not permit continued experiments with the hexagon PE single crystals. Needless to say, more work must be done to conclude anything concrete.

Moving away from polyethylene, other polymers can also be studied. Of particular interest to the polymer community is question if the glass transition temperature (T_g) changes with the thickness of thin PS films. Keddie, Jones and Cory[5] were the first to observe that T_g depends on the thickness of spin-cast PS thin films. Using ellipsometry, they found that T_g decreases substantially below the bulk value when films are less than 40 nm. Forrest and coworkers, using nulling ellipsometry, found that for free-standing films which have thickness less than 60 nm, T_g decreases by as much as ~70 ^{o}C.[6] Recently, Fryer, Nealy, and de Pablo[7], used a new technique called local thermal analysis using a thermal probe in contact with the PS to observe that T_g decreases by as

much as 25 ^{o}C below bulk for films 13 nm thick. Much discussion has occurred in the polymer community with regards to this phenomenon. We can contribute to the discussion by using our nanocalorimeter to characterize PS thin films. A possible experiment to conduct with our method would be to spin-cast PS thin films (at different thicknesses) onto the heater side of our calorimeters and perform measurements to observe T_g.

List of References

[1] Zhou, H.; Wilkes, G.L., Polymer 1997, 38, 5735.

[2] Leung, W.M.; Manley, R.St.J.; Panaras, A.R., Macromolecules 1985, 18, 750.

[3] Weaver, T.J.; Harrison, I.R., Polymer 1981, 22,1590.

[4] Nakagawa, Y.; Hayashi, H.; Takahagi, H.; Soeda, F.; Ishitani, A.; Toda, A.; Miyaji, H., Jpn. J. Appl. Phys. 1994, 33, 3771.

[5] Keddie, J.L.; Jones, R.L.; Cory, R.A., Europhys. Lett. 1994, 27, 59.

[6] Forrest, J. A.; Dalnoki, V.K.; Stevens, J. R.; Dutcher, J. R., Phys Rev. Lett. 1996, 77, 2002.

[7] Fryer, D.S.; Nealey, P.F.; de Pablo, J.J., Macromolecules 2000, 33, 6439.

VI. SUMMARY

In summary, a nanocalorimeter was used to study the melting of polyethylene single crystals. Preliminary experiments used a simple Ni-foil calorimeter, which replicates the nanocalorimeter on a macro-scale to demonstrate the feasibility of the technique using a PE film as the sample. Small amounts of isolated polyethylene crystals grown from solution were then studied using the nanocalorimeter. The melting temperature, which, previously, has not been determined by calorimetry, and the heat of fusion have been measured with good confidence using this technique. With this technique the detection of the melting of as few as 25 crystals is possible. Future work with probing of one single crystal may be possible with a redesign of the sensor. Future work will also include investigating the effect of annealing on the thermodynamics of the polyethylene single crystal system, the possible thickness-dependent melting point depression of PE single crystals, and the glass transition temperature of polystyrene.